J/ψ-N center of mass energy dependence of nuclear absorption effect on J/ψ production*

WANG Hong-Min(王宏民)[1;1)] HOU Zhao-Yu(侯召宇)[2] LIU Jia-Fu(刘家福)[1] SUN Xian-Jing(孙献静)[3]

[1] Physics Department, Academy of Armored Forces Engineering of PLA, Beijing 100072, China
[2] Physics Graduate School, Shijiazhuang Railway Institute, Shijiazhuang 050043, China
[3] Institute of High Energy Physics, Chinese Academy of Sciences, Beijing 100049, China

Abstract In this paper, the J/ψ nuclear absorption effect is studied at RHIC and LHC energies with the EKS98 shadowing parameterizations. By assuming that the J/ψ absorption cross section, σ_{abs}, increases with the charmonium-nucleon (J/ψ-N) center of mass energy, $\sqrt{s_{\mathrm{J/\psi N}}}$, it is found that σ_{abs} should depend on x_{F} (or y) at a certain center of mass energy per nucleon pair, $\sqrt{s}$, especially at LHC energies. The theoretical results with the x_{F} (or y)-dependence of the absorption effect are in good agreement with the experiment data from PHENIX in d-Au collisions and the predicted results will be examined by the forthcoming experimental data from LHC in d-Pb collisions. Finally, we also present baseline calculations of cold nuclear matter effects on J/ψ production in nucleus-nucleus (A-A) collisions and find that the x_{F} (or y)-dependence of absorption effect is very small at both RHIC and LHC energies in A-A collisions.

Key words x_{F} (or y)-dependence of absorption effect, NRQCD model, shadowing

PACS 24.85.+p, 25.75.-q, 12.38.Bx

1 Introduction

The charmonium state production, which is always used as a tool to probe the medium produced in nucleus-nucleus collisions, is an on-going major subject on both the experimental and theoretical sides. Recently, the results from the PHENIX experiment show a significant suppression of the J/ψ yield in Au-Au collisions at $\sqrt{s}=200$ GeV [1]. The experiment indicates that J/ψ production should be sensitive to QGP formation, due to the competing effects such as color Debye screening suppression or the so-called recombination mechanism [2]. However, the interpretation relies on a good understanding and a proper subtraction of the Cold Nuclear Matter (CNM) effects. The CNM effects include nuclear shadowing, initial-state energy loss and multiple scattering, and final-state $c\bar{c}$ absorption (or dissociation), etc. In Ref. [3], the theoretical results show that the initial-state energy loss can be neglected at the Relativistic Heavy Ion Collider (RHIC) energies and only the shadowing and nuclear absorption effects are important, which make the J/ψ production in deuteron-gold (d-Au) collisions at the RHIC an ideal tool to study these two effects, especially the absorption effect.

Shadowing, which is a depletion of parton density in a nucleus at small momentum fraction, x, compared with that in a free nucleon, has been probed through deep inelastic scattering (DIS) experiments of leptons and neutrinos from nuclei. Recently, there have been two trials to obtain shadowing parameterizations from the existing world experimental data. The HKM (Hirai, Kumano and Miyama) [4] nuclear shadowing parameterizations are obtained by an χ^2 global analysis of experimental data without including the proton-nucleus Drell-Yan data, which are subject to corrections for energy loss. Thus, the HKM parameterizations are an ideal tool to study the energy loss effect[3, 5, 6]. Unfortunately, the HKM is a parametrization which shows a very modest gluon shadowing, and already saturates around $x=0.01$ [7]. In contrast, the EKS (Eskola, Kolhinen and Salgado) [8] parameterizations show larger shadowing and a stronger slope around 0.01. In this paper, we

Received 1 February 2009
* Supported by Natural Science Foundation of Hebei Province (A2008000421)
1) E-mail: whmw@sina.com.cn

use the EKS98 shadowing together with MRST (Martin, Roberts, Stirling, and Thorne) [9] parton distribution functions in a proton. The inhomogeneous shadowing effect [3, 6, 10], which means that shadowing should depend on the spatial position of the interacting parton within the nucleus, is also considered when we analyze the results as a function of the number of nucleon-nucleon collisions.

The nuclear absorption effect, which occurs in the final state of J/ψ production, is another important CNM effect. Recently, it was believed that the nuclear absorption cross-section, σ_{abs}, should increase with the charmonium-nucleon center of mass energy, $\sqrt{s_{\mathrm{J/\psi N}}}$. In previous work [11–13], $\sqrt{s_{\mathrm{J/\psi N}}}$ is simply taken as a constant at a certain center of mass energy per nucleon pair, $\sqrt{s}$, so the absorption cross-section, σ_{abs}, should only depend on $\sqrt{s}$. By calculation, it is found that the $\sqrt{s_{\mathrm{J/\psi N}}}$ has a rather wide coverage at certain $\sqrt{s}$ and depends strongly on x_{F} (or rapidity y), especially at the Large Hadron Collider (LHC) energies. Thus, the absorption cross-section, σ_{abs}, should also have a strong dependence on (x_{F} (or y)-dependence) at certain $\sqrt{s}$. Since the J/ψ production is more realistically considered as a combination of octet and singlet states in the non-relativistic quantum QCD (NRQCD) model [14], we use the NRQCD model in this paper.

2 Method

In the NRQCD model, the total J/ψ includes radiative decays of the χ_{cJ} states and hadronic decays of the ψ′. If the inhomogeneous shadowing effect is considered, the rapidity distributions of J/ψ's produced in d-A collisions at the impact parameter $\vec{b}$ should be [3, 15]

$$\frac{\mathrm{d}\sigma_{\mathrm{dA}}^{\mathrm{J/\psi,tot}}}{\mathrm{d}y\mathrm{d}^2\vec{b}\mathrm{d}^2\vec{b}_{\mathrm{B}}}=\frac{\mathrm{d}\sigma_{\mathrm{dA}}^{\mathrm{J/\psi,dir}}}{\mathrm{d}y\mathrm{d}^2\vec{b}\mathrm{d}^2\vec{b}_{\mathrm{B}}}+\sum_{J=0}^{2}B(\chi_{\mathrm{cJ}}\rightarrow \mathrm{J/\psi}X)\frac{\mathrm{d}\sigma_{\mathrm{dA}}^{\chi_{\mathrm{cJ}}}}{\mathrm{d}y\mathrm{d}^2\vec{b}\mathrm{d}^2\vec{b}_{\mathrm{B}}}+\frac{\mathrm{d}\sigma_{\mathrm{dA}}^{\psi'}}{\mathrm{d}y\mathrm{d}^2\vec{b}\mathrm{d}^2\vec{b}_{\mathrm{B}}}. \quad (1)$$

The rapidity distribution of charmonium state, C, in NRQCD is

$$\frac{\mathrm{d}\sigma_{\mathrm{dA}}^{C}}{\mathrm{d}y\mathrm{d}^2\vec{b}\mathrm{d}^2\vec{b}_{\mathrm{B}}}=\sum_{i,j}\int_0^1\mathrm{d}x_1\mathrm{d}x_2\delta\left[y-\frac{1}{2}\ln\left(\frac{x_1}{x_2}\right)\right]\times\int\mathrm{d}z_{\mathrm{A}}\mathrm{d}z_{\mathrm{B}}F_i^{\mathrm{d}}(x_1,\mu^2,\vec{b}_{\mathrm{B}},z_{\mathrm{B}})F_j^{\mathrm{A}}(x_2,\mu^2,\vec{b}+\vec{b}_{\mathrm{B}},z_{\mathrm{A}})\times\hat{\sigma}(ij\rightarrow C), \quad (2)$$

where the C production cross section, $\hat{\sigma}(ij\rightarrow C)$, is given in Ref. [14], $\mu=2m_{\mathrm{c}}$ and the momentum fractions $x_{1,2}=\mu/\sqrt{s}\cdot\exp(\pm y)$.

In Eq. (2), the nuclear parton densities for gold (lead), $F_j^{\mathrm{A}}(x,\mu^2,\vec{b}_{\mathrm{A}},z_{\mathrm{A}})$, are the product of the nucleon density in the nucleus, $\rho_{\mathrm{A}}(r')$, and a shadowing ratio, $S_{P,\rho}^{j}(A,x,\mu^2,\vec{b}_{\mathrm{A}})$, where $\vec{b}_{\mathrm{A}}(=\vec{b}+\vec{b}_{\mathrm{B}})$ and z_{A} are the transverse and longitudinal locations of the parton in position space. The shadowing effect of the deuteron is ignored. Thus,

$$F_i^{d}(x,\mu^2,\vec{b}_{\mathrm{B}},z_{\mathrm{B}})=\rho_d(r)f_i^{\mathrm{N}}(x,\mu^2), \quad (3)$$

$$F_j^{\mathrm{A}}(x,\mu^2,\vec{b}_{\mathrm{A}},z_{\mathrm{A}})=\rho_{\mathrm{A}}(r')S_{P,\rho}^{j}(A,x,\mu^2,\vec{b}_{\mathrm{A}})f_j^{\mathrm{N}}(x,\mu^2), \quad (4)$$

where $r=\sqrt{\vec{b}_{\mathrm{B}}^2+z_{\mathrm{B}}^2}$ and $r'=\sqrt{\vec{b}_{\mathrm{A}}^2+z_{\mathrm{A}}^2}$. The deuteron density distribution is given by the Húlthen form [16], and the nucleon densities of gold (lead) are parameterized by a Fermi distribution [17]. The ratio for the spatial dependence of shadowing is [3,18]

$$S_{P,\rho}^{j}(A,x,\mu^2,\vec{b}_{\mathrm{A}})=1+N_\rho(S_P^{j}(A,x,\mu^2)-1)\frac{\int\mathrm{d}z\rho_{\mathrm{A}}(\vec{b}_{\mathrm{A}},z)}{\int\mathrm{d}z\rho_{\mathrm{A}}(0,z)}, \quad (5)$$

where N_ρ is chosen so that

$$\int\mathrm{d}^2\vec{b}_{\mathrm{A}}\mathrm{d}z_{\mathrm{A}}\rho_{\mathrm{A}}(r')S_{P,\rho}^{j}(A,x,\mu^2,\vec{b}_{\mathrm{A}})=S_P^{j}(A,x,\mu^2).$$

Because the $\mathrm{c\bar{c}}$ pair may interact with nucleons and be dissociated or absorbed before it can escape the target, the production cross section in Eq. (1) should be weighted by the survival probability, S_{abs}, and

$$S_{abs}(\vec{b}_{\mathrm{A}},z_{\mathrm{A}})=\exp\left\{-\int_{z_{\mathrm{A}}}^{\infty}\mathrm{d}z'_{\mathrm{A}}\rho_{\mathrm{A}}(\vec{b}_{\mathrm{A}},z'_{\mathrm{A}})\sigma_{abs}(z'_{\mathrm{A}}-z_{\mathrm{A}})\right\}, \quad (6)$$

where z_{A} is the longitudinal production point of the $\mathrm{c\bar{c}}$ pair and z'_{A} is the point at which the state is absorbed. In NRQCD, J/ψ production is more realistically considered as a combination of octet and singlet states. For the octet absorption cross section, $\sigma_{abs}^{\mathrm{o}}$, established at the production of the state, it is independent of the position $z_{\mathrm{A}}(z'_{\mathrm{A}})$. If the $\mathrm{c\bar{c}}$ pair is produced as a color singlet, it is initially small with a spatial extent on the order of its production time, τ. The growth of the absorption cross section is accordingly given by [15]

$$\sigma_{abs}^{\mathrm{s}}(z'_{\mathrm{A}}-z_{\mathrm{A}})=\begin{cases}\sigma_{\psi_{\mathrm{i}}\mathrm{N}}^{\mathrm{s}}\left(\dfrac{\tau}{\tau_{\psi_{\mathrm{i}}\mathrm{N}}}\right)^{k} & \text{if } \tau<\tau_{\psi}\\ \sigma_{\psi_{\mathrm{i}}\mathrm{N}}^{\mathrm{s}} & \text{otherwise,}\end{cases} \quad (7)$$

where the proper time τ is related to the path length traversed by the $\mathrm{c\bar{c}}$ pair through nuclear matter,

$\tau=(z'_{\rm A}-z_{\rm A})/\gamma v$ [15]. The γ factor introduces $x_{\rm F}$ and energy dependences in the growth of the cross section. In this paper, the value of $\sigma^{\rm s}_{{\rm J}/\psi{\rm N}}$ is simply taken as $\sigma^{\rm s}_{{\rm J}/\psi{\rm N}}=\sigma^{\rm o}_{{\rm J}/\psi{\rm N}}=\sigma_{abs}$, and the asymptotic absorption cross section scale is assumed in proportion to the squares of the charmonium raddi, $\sigma^{\rm s}_{\psi'{\rm N}}=3.7\sigma^{\rm s}_{{\rm J}/\psi{\rm N}}$ and $\sigma^{\rm s}_{\chi_{\rm cJ}{\rm N}}=2.4\sigma^{\rm s}_{{\rm J}/\psi{\rm N}}$ [15].

In this paper, since the $c\bar{c}$ pair can be more easily absorbed with the increasing charmonium-nucleon center of mass energy (c. m. energy), we assume that the $c\bar{c}$ pair absorption section, σ_{abs}, should increase with the charmonium-nucleon c. m. energy

$$\sqrt{s_{{\rm J}/\psi{\rm N}}}=\sqrt{m^2_{c\bar{c}}+m^2_{\rm N}+2Em_{\rm N}}\approx\sqrt{2P_{c\bar{c}}}, \quad (8)$$

where $E(=\sqrt{m^2_{c\bar{c}}+P^2_{c\bar{c}}})$ is the energy of the charmonium in the rest frame of the nucleus. The momentum of the $c\bar{c}$ pair in the rest frame of the nucleus is [19]

$$P_{c\bar{c}}=\frac{s}{4m}\left(x_{\rm F}+\sqrt{x^2_{\rm F}+\frac{4m^2_{c\bar{c}}}{s}}\right), \quad (9)$$

where $x_{\rm F}=\mu/\sqrt{s}\cdot(\exp(y)-\exp(-y))$, $m_{c\bar{c}}$ is the charmonium mass and m is the nucleon mass. In Refs. [11–13], the $\sqrt{s_{{\rm J}/\psi{\rm N}}}$ is simply taken as $\sqrt{s_{0{\rm J}/\psi{\rm N}}}$, which is the $\sqrt{s_{{\rm J}/\psi{\rm N}}}$ at zero $x_{\rm F}$ (or y), and $\sqrt{s_{0{\rm J}/\psi{\rm N}}}=\sqrt{m_{c\bar{c}}\sqrt{s}}$ [13]. Therefore, the absorption cross section will only increase with $\sqrt{s}$ as

$$\sigma_{0abs}(\sqrt{s})=\sigma_{0abs}(\sqrt{s_0})\left(\frac{\sqrt{s}}{\sqrt{s_0}}\right)^{\delta}, \quad (10)$$

where $\sqrt{s_0}$ is taken as 200 GeV (the BNL RHIC energies). However, by Eqs. (8) and (9), it is found that the $\sqrt{s_{{\rm J}/\psi{\rm N}}}$ at LHC energies has a rather wide coverage, $\sqrt{s_{{\rm J}/\psi{\rm N}}}\approx 10-1000$ GeV, so it can not be taken as a constant again. In our work, the value of $\sqrt{s_{{\rm J}/\psi{\rm N}}}$ is considered as a variable at certain $\sqrt{s}$ and the effective absorption cross section is given by

$$\sigma_{abs}(\sqrt{s_{{\rm J}/\psi{\rm N}}})=\sigma_{0abs}(\sqrt{s})\left(\frac{\sqrt{s_{{\rm J}/\psi{\rm N}}}}{\sqrt{s_{0{\rm J}/\psi{\rm N}}}}\right)^{\delta}, \quad (11)$$

which should be a function of $x_{\rm F}$(or y) ($x_{\rm F}$ (or y)-dependence).

If the nuclear absorption effect is considered, the total J/ψ rapidity distributions produced in d-A collisions at the impact parameter $\vec{b}$ should be rewritten as [18]

$$\frac{{\rm d}\sigma^{{\rm J}/\psi,{\rm tot}}_{\rm dA}}{{\rm d}y{\rm d}^2\vec{b}{\rm d}^2\vec{b}_{\rm B}}=\left[\frac{{\rm d}\sigma^{{\rm J}/\psi,{\rm dir,o}}_{\rm dA}}{{\rm d}y{\rm d}^2\vec{b}{\rm d}^2\vec{b}_{\rm B}}+\sum_{J=0}^{2}B(\chi_{\rm cJ}\to{\rm J}/\psi X)\frac{{\rm d}\sigma^{\chi_{\rm cJ},{\rm o}}_{\rm dA}}{{\rm d}y{\rm d}^2\vec{b}{\rm d}^2\vec{b}_{\rm B}}+\frac{{\rm d}\sigma^{\psi',{\rm o}}_{\rm dA}}{{\rm d}y{\rm d}^2\vec{b}{\rm d}^2\vec{b}_{\rm B}}\right]S^{\rm o}_{abs}(\vec{b}_{\rm A},z_{\rm A})+$$
$$\left[\frac{{\rm d}\sigma^{{\rm J}/\psi,{\rm dir,s}}_{\rm dA}}{{\rm d}y{\rm d}^2\vec{b}{\rm d}^2\vec{b}_{\rm B}}S^{\rm dir,s}_{abs}(\vec{b}_{\rm A},z_{\rm A})+\sum_{J=0}^{2}B(\chi_{\rm cJ}\to{\rm J}/\psi X)\frac{{\rm d}\sigma^{\chi_{\rm cJ},{\rm s}}_{\rm dA}}{{\rm d}y{\rm d}^2\vec{b}{\rm d}^2\vec{b}_{\rm B}}S^{\chi_{\rm cJ},{\rm s}}_{abs}(\vec{b}_{\rm A},z_{\rm A})+\frac{{\rm d}\sigma^{\psi',{\rm s}}_{\rm dA}}{{\rm d}y{\rm d}^2\vec{b}{\rm d}^2\vec{b}_{\rm B}}S^{\psi',{\rm s}}_{abs}(\vec{b}_{\rm A},z_{\rm A})\right]. \quad (12)$$

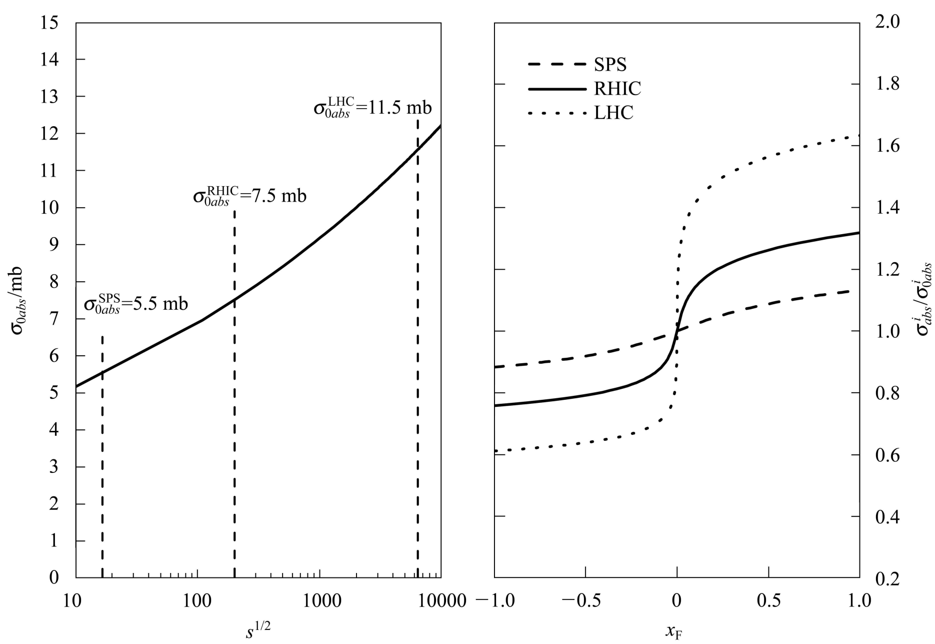

Fig. 1. Left-hand side: The energy dependence of σ_{0abs} versus $\sqrt{s}$ with Eq. (10). Right-hand side: The ratio of $\sigma^i_{abs}/\sigma^i_{0abs}$ versus $x_{\rm F}$ with Eq. (11) at different collision energies: RHIC (solid), SPS (dashed) and LHC (dotted).

3 Results and discussion

In Fig. 1, the left plot shows the collision energy dependence of σ_{0abs} versus $\sqrt{s}$ by Eq. (10) with $\delta=0.125$ [13]. By a χ^2 analysis [4, 5] of the experimental data given by PHENIX [20], with χ^2/(degree of freedom)=0.15, it is found that the value of the charmonium-nucleon absorption cross section at RHIC energies $\sigma_{0abs}^{\rm RHIC}=7.5$ mb. Correspondingly, the absorption cross section, σ_{0abs}, at the Super Proton Synchrotron (SPS) and LHC energies will be 5.5 mb and 11.5 mb, respectively. The right plot is the ratio of $\sigma^i_{abs}/\sigma^i_{0abs}$ versus $x_{\rm F}$ with Eq. (11) at different collision energies: RHIC (solid), SPS (dashed) and LHC (dotted). It is shown that the absorption cross section at LHC energies has stronger $x_{\rm F}$ (or y)-dependence than that at RHIC or SPS energies.

In order to compare with the experimental data from PHENIX [20], we introduce the nuclear modification factor

$$R_{\rm dAu}=\frac{{\rm d}\sigma^{\psi,{\rm tot}}_{\rm dAu}/{\rm d}y}{{\rm d}\sigma_{\rm pp}/{\rm d}y}, \tag{13}$$

where

$$\frac{{\rm d}\sigma^{\psi,{\rm tot}}_{\rm dAu}}{{\rm d}y}=\int{\rm d}^2\vec{b}{\rm d}^2\vec{b}_{\rm B}\frac{{\rm d}\sigma^{\psi,{\rm tot}}_{\rm dA}}{{\rm d}y{\rm d}^2\vec{b}{\rm d}^2\vec{b}_{\rm B}}.$$

The J/ψ ratios of dAu/pp at 200 GeV versus rapidity with the EKS98 shadowing are presented in Fig. 2. The solid curve is observed by the inhomogeneous shadowing effect without nuclear absorption. The dashed and dotted curves correspond to $\sigma_{abs}=\sigma^{\rm RHIC}_{0abs}$ and $\sigma^{\rm RHIC}_{0abs}\left(\frac{\sqrt{s_{{\rm J}/\psi{\rm N}}}}{\sqrt{s_{0{\rm J}/\psi{\rm N}}}}\right)^{\delta}$ ($x_{\rm F}$ (or y)-dependence of absorption effect) together with the inhomogeneous shadowing effect, respectively. Fig. 3 shows the $R_{\rm dAu}(b)$ ratios for the same rapidity values as a function of the number of binary NN collisions $N_{\rm coll}(b)=\sigma_{\rm in}\int{\rm d}^2\vec{b}_{\rm B}T_{\rm B}(b_{\rm B})T_{\rm A}(|\vec{b}+\vec{b}_{\rm B}|)$, and the ratio $R_{\rm dAu}(b)$ is defined as

$$R_{\rm dAu}(b)=\frac{1}{N_{\rm coll}(b)}\frac{\int{\rm d}y{\rm d}^2\vec{b}_{\rm B}\frac{{\rm d}\sigma_{\rm dAu}}{{\rm d}y{\rm d}^2\vec{b}{\rm d}^2\vec{b}_{\rm B}}}{\int{\rm d}y\frac{{\rm d}\sigma_{\rm pp}}{{\rm d}y}}\ . \tag{14}$$

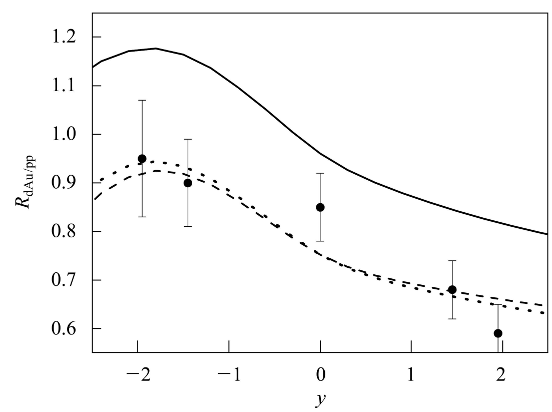

Fig. 2. The minimum bias $R_{\rm dAu}$ versus rapidity with the EKS98 shadowing parametrization at RHIC energies. The curves are $\sigma_{abs}=0$ (solid), $\sigma^{\rm RHIC}_{0abs}$ (dashed) and $\sigma^{\rm RHIC}_{0abs}\left(\frac{\sqrt{s_{{\rm J}/\psi{\rm N}}}}{\sqrt{s_{0{\rm J}/\psi{\rm N}}}}\right)^{\delta}$ (dotted). The experimental data are taken from PHENIX [20].

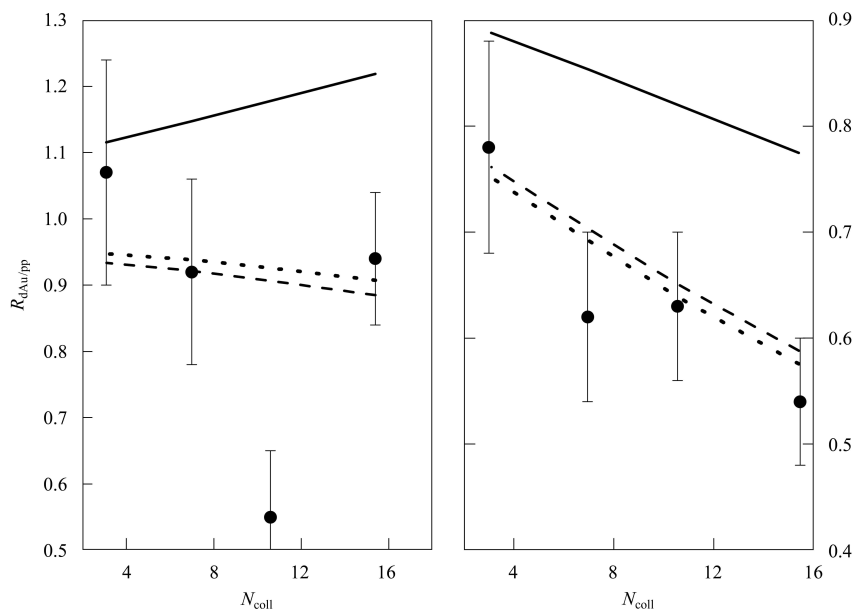

Fig. 3. The $R_{\rm dAu}(b)$ ratios with the EKS98 shadowing parametrization versus $N_{\rm coll}$ for different rapidity ranges: $-2.2<y<-1.2$ (a) and $1.2<y<2.2$ (b). The figure comments are the same as Fig. 2.

The integral rapidity ranges are $-2.2 < y < -1.2$ (a) and $1.2 < y < 2.2$ (b) with the same figure captions as Fig. 2. It is shown that the theoretical results with $x_{\rm F}$ (or y)-dependence of absorption effect (dotted curve) are in better agreement with the experimental data than those simply taking the absorption cross-section as $\sigma_{0abs}^{\rm RHIC}$ (dashed curve) in both Fig. 2 and Fig. 3.

In order to predict the new experimental results at the LHC, the theoretical results of the ratio for dPb/pp at 6.2 TeV with EKS98 shadowing are shown in Fig. 4(a) ($y = -3.5$) and Fig. 4(b) ($y = 3.5$). The solid and dashed curves correspond to the results for $\sigma_{abs} = \sigma_{0abs}^{\rm LHC}$ and $\sigma_{0abs}^{\rm LHC}\left(\frac{\sqrt{s_{\rm J/\psi N}}}{\sqrt{s_{\rm 0J/\psi N}}}\right)^{\delta}$ ($x_{\rm F}$ (or y)-dependence of absorption effect) together with the inhomogeneous shadowing effect, respectively. Because the absorption cross section at LHC energies has stronger $x_{\rm F}$ (or y)-dependence than that at RHIC energies, the $x_{\rm F}$ (or y)-dependence of absorption effect at LHC energies is more obvious than that at RHIC, as shown in Fig. 3.

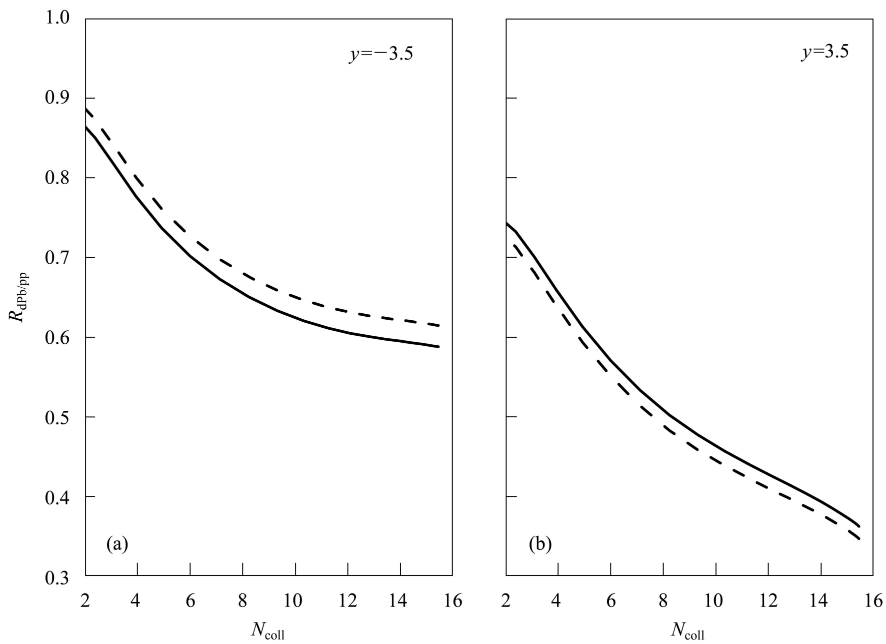

Fig. 4. The $R_{\rm dPb}(b)$ ratios with the EKS98 shadowing parametrization versus $N_{\rm coll}$ at LHC energies with $y = -3.5$ (a) and $y = 3.5$ (b). The curves are $\sigma_{abs} = \sigma_{0abs}^{\rm LHC}$ (solid) and $\sigma_{0abs}^{\rm LHC}\left(\frac{\sqrt{s_{\rm J/\psi N}}}{\sqrt{s_{\rm 0J/\psi N}}}\right)^{\delta}$ (dashed).

Finally, we present the baseline calculations of CNM effects on J/ψ production in nucleus-nucleus (A-A) collisions at RHIC and LHC energies. The AA/pp ratios with the EKS98 shadowing as a function of y at RHIC (a) and LHC (b) energies are shown in Fig. 5. The figure captions are the same as in Fig. 2. It is shown that the results when considering the $x_{\rm F}$ (or y)-dependence of absorption effect (dotted curve) are almost the same as the results without considering this effect (dashed curve) in both Fig. 5(a) and Fig. 5(b). Since $R_{\rm AA}(y)$ can be seen as $R_{\rm dA}(-y) \times R_{\rm dA}(+y)$, the AA/pp ratios versus y have an approximate symmetry about $y = 0$ [21] and the $x_{\rm F}$ (or y)-dependence of absorption effect can be neglected at both RHIC and LHC energies on J/ψ production in A-A collisions as shown in Fig. 5.

In summary, the $x_{\rm F}$ (or y)-dependence of absorption is studied at the RHIC and LHC energies. At RHIC and LHC energies, the $x_{\rm F}$ (or y)-dependence of nuclear absorption effect is verified to be important, and the theoretical results will be examined by the forthcoming experimental data from LHC. The value of δ[1], which is not given exactly, should also be determined by the forthcoming experimental data.

1) The value of δ is taken as 0.16 in Ref. [11], 0.4 in Ref. [12] and 0.125 in Ref. [13].

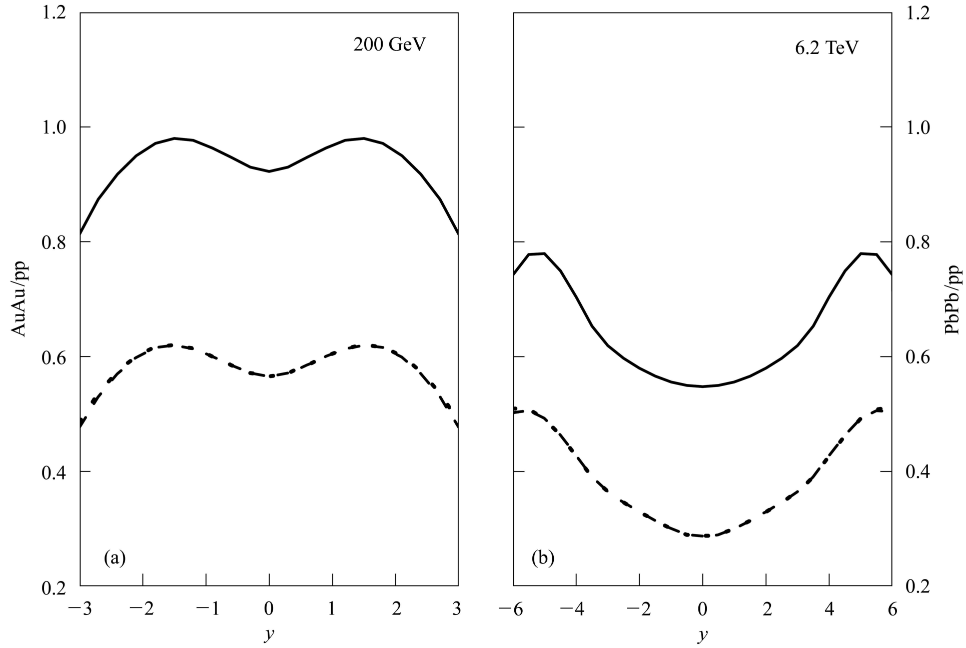

Fig. 5. Left-hand side: The ratios of AuAu/pp with EKS98 shadowing at RHIC energies versus rapidity for $\sigma_{abs}=0$ (solid), $\sigma_{0abs}^{\rm LHC}$ (dashed) and $\sigma_{0abs}^{\rm LHC}\left(\frac{\sqrt{s_{\rm J/\psi N}}}{\sqrt{s_{\rm 0J/\psi N}}}\right)^{\delta}$ (dotted). Right-hand side: The ratio of PbPb/pp at LHC energies; the figure comments are the same as the left one.

References

1 Adare A, Afanasiev S, Aidala C et al. Phys. Rev. Lett., 2007, **98**: 232301

2 YAN L, ZHUANG P F, XU N. Phys. Rev. Lett., 2006, **97**: 232301; Andronic A, Braun M P, Redlich K et al. Nucl. Phys. A, 2007, **789**: 334–356; Capella A, Bravina L, Ferreiro E G et al. hep-ph/0712.4331

3 WANG H M, HOU Z Y, SUN X J. Chin. Phys. C (HEP& NP), 2008, **32**(11): 892–896

4 Hirai M, Kumano S, Miyama M. Phys. Rev. D, 2001, **64**: 034003; Hirai M, Kumano S, Nagai T H. Phys. Rev. C, 2004, **70**: 044905

5 DUAN C G, SONG L H, HUO L J et al. Eur. Phys. J. C, 2003, **29**: 557–561

6 WANG H M, SUN X J, ZHANG B A. Phys. Scr., 2007, **75**: 651–655

7 Eskola K J, Paukkunena H, Salgadoc C A. hep-ph/0802.0139

8 Eskola K J, Kolhinen V J, Salgado C A. Eur. Phys. J. C, 1999, **9**: 61–68

9 Martin A D, Roberts R G, Stirling W J et al. Eur. Phys. J. C, 2005, **39**: 155–161

10 Emel'yanov V, Khodinov A, Klein S R et al. Phys. Rev. C, 2000, **61**: 044904

11 Armesto N, Braun M A, Capella A, Pajares C et al. Nucl. Phys. B, 1998, **509**: 357–377

12 HE Y B, Hufner J, Kopeliovich B Z. Phys. Lett. B, 2000, **477**: 93–98

13 Bedijdian M, Blaschke D, Bodwin G T et al. hep-ph/0311048

14 Beneke M, Rothstein I Z. Phys. Rev. D, 1996, **54**: 2005–2016

15 Vogt R. Phys. Rev. C, 2000, **61**: 035203

16 Kharzeev D, Levin E M, Nardi M. Nuclear Physics. A, 2004, **730**: 448–459; Húlthen L, Sagawara M. Handbüch der Physik, 1957, **39**

17 de Vries H, de Jager C W, de Vries C. Atomic Data and Nuclear Data Tables, 1987, **36**: 495–536

18 Vogt R. Phys. Rev. C, 2005, **71**: 054902

19 Kharzeev D, Satz H. Phys. Lett. B, 1993, **334**: 389–396

20 Adare A, Adler S S, Afanasiev S et al. Phys. Rev. C, 2008, **77**: 024912

21 Ferreiro E G, Fleuret F, Lansberg J P et al. hep-ph/0809.4684